WELDING RESEARCH

SUPPLEMENT TO THE WELDING JOURNAL, FEBRUARY 1986

Sponsored by the American Welding Society and the Welding Research Council

Gas/Metal/Slag Reactions in Submerged Arc Welding Using $CaO-Al_2O_3$ Based Fluxes

Separation of deoxidized products into the slag significantly affects the levels of oxygen and aluminum in the weld metal

BY T. LAU, G. C. WEATHERLY AND A. MC LEAN

In this paper, a detailed study is presented of the interactions of Mn, Al and O at the different stages of the welding operation. These interactions have been studied by analyzing the total Mn, Al and O contents, as well as the composition of inclusions formed at the different stages. At the electrode tip and in the arc column, changes in oxygen, aluminum and manganese were dominated by flux decomposition, while at the weld metal stage, slag-metal reactions occurred. These reactions were most extensive in MnO-containing fluxes, and resulted in a significant loss of oxygen, as well as metallic species such as aluminum, by the separation of oxidized products into the slag phase. In the $CaF_2-Al_2O_3$ containing flux studied, reactions involving CaF_2, Al_2O_3 and dissolved Al and Si led to enhanced Al pickup at the electrode tip. The applicability of equilibrium thermodynamic arguments to welding was assessed by determining the effective temperatures for the pertinent equilibrium reactions. These temperatures were found to be in reasonable agreement with other values in the literature. However, it is the efficiency of inclusion separation to the slag that determines the effective temperature.

T. LAU is with the Welding Institute of Canada, Oakville, Ontario. G. C. WEATHERLY and A. MC LEAN are with the Department of Metallurgy and Materials Science, University of Toronto, Toronto, Ontario.

Introduction

In a previous study conducted by Lau, Weatherly and McLean (Ref. 1), the major sources of oxygen and nitrogen contamination during submerged arc welding were elucidated by studying three stages of the welding process, *i.e.*, the electrode tip stage, the droplet stage and the weld metal stage. One of the most significant findings was the very high oxygen levels in the droplets (> 1400 ppm). This emphasizes the importance of reactions within the arc column. On the other hand, the oxygen levels in the final weld metal were very much lower (< 700 ppm), even after allowing for dilution effects from the base plate, and this suggests that slag-metal interactions must be important in determining the final oxygen level in the weld metal. In this paper, the results are presented of a detailed analysis of inclusion compositions and aluminum and manganese levels at the three stages noted above. This information, together with the trends shown by the oxygen results, has been used to assess the relative importance of the different sources of oxygen contamination and to consider the question of slag-metal equilibrium in welding.

Several potential sources of oxygen contamination in submerged arc welding can be postulated:

1. Entrapment of molten flux particles by weld metal droplets.
2. Decomposition of flux components in the arc column, with subsequent gas-metal reactions.
3. Air entrapment within the porous flux particles.
4. Slag-metal reactions.

If entrapped flux particles are a significant source of contamination, one might

Table 1—Compositions of Base Plate, Wire and Flux Used in the Study

	C	Mn	Si	S	P	Mo	Cr	Al	O
Base Plate	0.07	1.79	0.23	0.03	0.008	0.14	0.21	0.024	0.004
Wire	0.11	1.06	0.27	0.017	0.0025	–	–	0.006	0.016

Flux	CaO	CaF_2	Al_2O_3	MnO	SiO_2	MgO
L1	72.5[a]		26.7	–	–	0.8
L2	42.3		32.4	25.3	–	–
L3	37.1		32.0	–	24.7	6.2
L4	39.8		36.5	13.0	10.6	–
L5	96.4[a]		–	–	–	3.6

[a]Only Ca was determined by x-ray fluorescence analysis. Flux L1 contained 37.5 wt-% CaO, 25 wt-% CaF2 and 37.5 wt-% Al_2O_3, while Flux L5 contained 25 wt-% CaO and 75 wt-% CaF_2 prior to melting.

expect to find inclusions with compositions close to that of the flux. On the other hand, if substantial decomposition of the flux occurs, there is no reason to believe that the inclusion composition would be the same as that of the flux. Air entrapment as a potential source of oxygen contamination was considered in the previous study (Ref. 1). There it was shown that this source plays only a minor role in the overall picture.

The majority of previous studies have concentrated on the role of slag-metal reactions and the assumption of equilibrium in the weld pool. One of the first attempts to describe the influence of the slag phase in terms of a flux Basicity Index (B. I.) was by Tuliani, *et al.* (Ref. 2). This gave a reasonable correlation with the weld metal oxygen values. However as North, *et al.* (Ref. 3), have shown, the basicity of a slag reflects the concentration of oxygen ions in the molten slag, and this can be quite different from the oxidizing power of the slag. Furthermore, the Basicity Index ignores the interactions that occur between components of the flux and is really an empirical parameter. Eager (Ref. 4) proposed that the Basicity Index/oxygen relationship should be replaced by equilibrium curves for the $SiO_2 = Si + 2O$ reaction at B. I. values <2, and by the $FeO = Fe + O$ reaction at B. I. values >2. He suggested that the existing data were consistent with a reaction temperature of 2000°C (3632°F), but other authors, *e.g.*, Davis and Coe (Ref. 5), selected 1650°C (3002°F) as the effective reaction temperature.

It is debatable whether the concept of true thermodynamic equilibrium is useful in welding studies in view of the short reaction times (<1 s) before the weld pool freezes and the very rapid thermal cycle experienced by the molten metal. However, the weld pool is well stirred prior to freezing, and the extremely fast metal-slag reaction rates shown by the work of Caryll and Ward (Ref. 6) at 1600°C (2912°F) suggest that extensive metal-slag reactions will occur even within the limited reaction times available. If equilibrium is attained at any temperature, the final oxygen value in the weld metal will depend not only on equilibrium considerations, but also the extent to which the immiscible reaction products formed at higher temperatures can separate into the slag phase prior to freezing. This aspect was used by Tuliani, *et al.* (Ref. 7), to explain the formation of clean welds using carbonate fluxes. Despite the high oxidizing power of a carbonate flux, the final weld was low in oxygen because the products of deoxidation nucleated readily and separated out prior to freezing.

The results of previous tests (Ref. 1) have demonstrated the importance of reactions at the weld tip and in the arc column. Other studies have also suggested that events occurring at the electrode tip are important (Refs. 3, 8, 9). However, if extensive slag-metal reactions can occur in the weld pool and the deoxidation products can be removed prior to freezing, reactions at the earlier stages would only be important in determining the levels of other elements, *e.g.*, Al, Mn and Si, involved in the process. The excess oxygen carried into the weld pool by the droplets would form inclusions at a relatively high temperature, which should then separate into the slag.

Table 2—Analysis of Inclusions Observed at Different Stages of Welding (at 300 A)

Inclusion Chemistry (wt-%)	Electrode Tip Inclusion Type 1	2	3	Weld Metal Droplet Inclusion Type 1	2	3	Weld Metal Inclusion Type 1	2	3
Flux L1									
Al_2O_3		2			7	13	70		84
MnO		58	54		50	48	2		16
SiO_2		40	46		43	38			
CaO	–	–	–	–	–	–	28		
Flux L2	10%[a]	90%[a]		35.5%[a]	64.5%[a]		1%	99[a]	
Al_2O_3	13	4		17	6	4	10	4	
MnO	34	58	63	51	75	75	63	75	75
SiO_2	40	38	37	18	19	30	21	21	24
CaO	13	–	–	14			6		
Flux L3	11%[a]	89%[a]		37.5%[a]	62.5%[a]		54.5%[a]	45.5%[a]	
Al_2O_3	19	5		12	6	6	23	37	26
MnO	19	56	39	25	50	55	16	37	45
SiO_2	34	39	58	45	44	39	35	26	28
CaO	38		3	18			26		
Flux L4				44%[a]	56%[a]		62%[a]	38%[a]	
Al_2O_3	14	2		19	13		15	12	6
MnO	34	56	60	28	51	58	39	55	59
SiO_2	34	42	40	37	36	42	35	32	30
CaO	18			16			11		
Flux L5				15%[a]	85%[a]				
Al_2O_3							8		9
MnO		45	30	37	52	57	34		38
SiO_2		53	66	37	48	40	41		51
CaO				26			17		

[a]Relative amounts of Type 1 and Type 2 inclusions only.
Notes: 1) Trace amounts of MgO were found in some of the inclusions, and those have been included in the CaO content where appropriate. 2) Some of the inclusion compositions do not add up to 100%, e.g., Flux L5. The balance in each case was due to the presence of S.

Experimental Procedure

Five synthetic laboratory fluxes were used for this study. The composition of the fluxes, together with the wire and base plate compositions, are given in Table 1. A description of the preparation of the fluxes, welding procedures and analysis of the electrode tips, weld metal droplets and weld metal was given in the previous study (Ref. 1). All welds were made either at 300 or 600 A with the same heat input.

The total Al and Mn contents of the samples were analyzed by neutron activation analysis. A sample weighing about 0.5 g (0.018 oz) was irradiated for 30 s at an energy level of 2 kW (10^{11} neutrons/

cm^2s). After a delay time of 60 s, the radioactivity of the sample was counted for 100 s using an x-ray counter. The aluminum and manganese levels were then calculated by comparing the results with those obtained from standard samples irradiated under identical conditions. The accuracy of the reported values is estimated to be ±3%. The total oxygen content of the samples was determined by inert gas fusion analysis. The silicon content of the weld metal was determined by standard spectrographic techniques for the 300 A samples only.

An SEM equipped with an EDX attachment was used to analyze the composition of the inclusions at the three stages. A quantitative computer program was used to determine the weight percentages of the oxide components, assuming that they form the most stable oxides in the inclusion. The accuracy of this program is estimated to be about ±5% for each oxide composition. For the smallest inclusions (1 μm in size or smaller), some interference from the surrounding iron matrix complicated the analysis. To avoid contamination by the iron matrix, these inclusions were extracted on a carbon replica and their composition was rechecked. On no occasion was any iron signal detected from these small inclusions.

In order to assess the change in composition between the falling droplet and the weld metal, it was necessary to determine the dilution factor by geometric measurement of sections removed from the welds.

Table 3—Analysis of Inclusions Observed at Different Stages of Welding (at 600 A)

Inclusion Chemistry (wt-%)	Electrode Tip Inclusion Type 1	2	3	Weld Metal Droplet Inclusion Type 1	2	3	Weld Metal Inclusion Type 1	2	3
Flux L1				13.3%[a]	86.7%[a]				
Al_2O_3	–	1.0	–	20	5	6	64	–	86
MnO	–	60	45	11	58	58	–	–	14
SiO_2	–	39	55	30	37	34	–	–	–
CaO	–			39	–	–	35	–	–
Flux L2	22.7%[a]	77.3%[a]		33.3%[a]	66.7%[a]		36.8%[a]	63.2%[a]	
Al_2O_3	21	19	3	20	8	5	10	4	–
MnO	23	55	50	41	64	67	53	69	71
SiO_2	32	35	43	25	28	27	30	27	26
CaO	25	–	–	14	–	–	7	–	–
Flux L3	35%[a]	65%[a]	–	46.2%[a]	53.8%[a]		59.1%[a]	40.8%[a]	
Al_2O_3	13	17	6	14	8	2	18	28	25
MnO	26	48	51	10	48	51	22	43	41
SiO_2	40	35	43	45	44	47	40	29	27
CaO	21	–	–	31	–	–	20	–	–
Flux L4	35%[a]	65%[a]		50%[a]	50%[a]		70%[a]	30%[a]	
Al_2O_3	16	4	11	23	3	5	16	11	11
MnO	28	56	52	16	57	59	33	53	53
SiO_2	37	40	37	36	40	36	35	36	30
CaO	19	–	–	25	–	–	16	–	–

[a]Relative amounts of Type 1 and Type 2 inclusions only.
Notes: 1) Trace amounts of MgO were found in some of the inclusions, and those have been included in the CaO content where appropriate. (2) Some of the inclusion compositions do not add up to 100%, *e.g.*, Flux L5. The balance in each case was due to the presence of S.

Results

Inclusion Analysis

The average compositions of the inclusions observed at the three stages are shown in Table 2 (300 A) and Table 3 (600 A) for the five fluxes listed in Table 1. At least 80 inclusions were analyzed at each stage, and they were classified into one of three groups, depending on their size and composition. Type 1 and Type 2 inclusions ranged in size from several microns to 100 microns in diameter. Type 1 inclusions contained CaO, while Type 2 inclusions did not. The relative abundance of these two types of inclusions, which because of their size make the major contribution to the measured oxygen values, was also determined, and these results are included in Tables 2 and 3. Type 3 inclusions were much smaller in size, ≤1 μm in diameter, and are believed to be the products of deoxidation formed just before the weld pool freezes. There was considerable variation in the composition of the inclusions at all stages, particularly those found in the weld droplets and electrode tips. As an example of this variability, Table 4 lists the individual readings of the compositions of 25 Type 1 inclusions, ranging from 5 to 60 μm in size, observed in droplets deposited with Flux L4 at 600 A.

There was also some variability in the levels of the major elements from one location to the next within a single inclusion. Typically, the Mn content was lower at the center and higher at the periphery of all the larger inclusions, while the Al content showed the opposite trend—Fig. 1. No marked variation was noted in the Si levels from center to edge.

Table 4—Results of Inclusion Analysis of Type 1 Particles Observed in Droplets Deposited with Flux L4 (at 600 A)

Size (μm)	Al_2O_3 wt-%	MnO wt-%	SiO_2 wt-%	CaO wt-%
50	31.0	2.7	25.6	40.6
60	35.1	0.0	26.0	38.8
60	31.8	4.8	28.8	34.9
25	28.7	4.1	34.5	32.4
24	24.7	8.8	36.4	29.9
30	23.3	15.4	32.7	28.6
23	24.1	14.5	34.1	27.3
28	28.2	10.7	35.3	25.8
37	24.0	15.5	36.1	24.3
16	18.9	20.4	37.0	23.7
11	18.2	21.8	37.6	22.2
18	18.1	18.8	41.8	21.2
11	19.3	18.4	41.3	20.8
16	18.5	27.6	33.8	19.9
20	20.0	19.3	41.0	19.5
10	18.0	22.5	37.9	18.2
21	11.5	33.0	39.1	16.4
17	15.4	29.7	40.7	14.2
9	9.8	38.4	38.2	13.3
8	8.8	36.7	42.1	12.1
14	15.6	28.4	43.8	12.0
5	11.2	40.4	37.2	11.0
9	26.3	31.0	34.2	8.2
8	26.1	29.9	35.9	8.0
10	25.5	30.7	35.8	8.0

Mn and Al Analysis

The results of the analyses of Mn and Al (and also O) at the three stages of

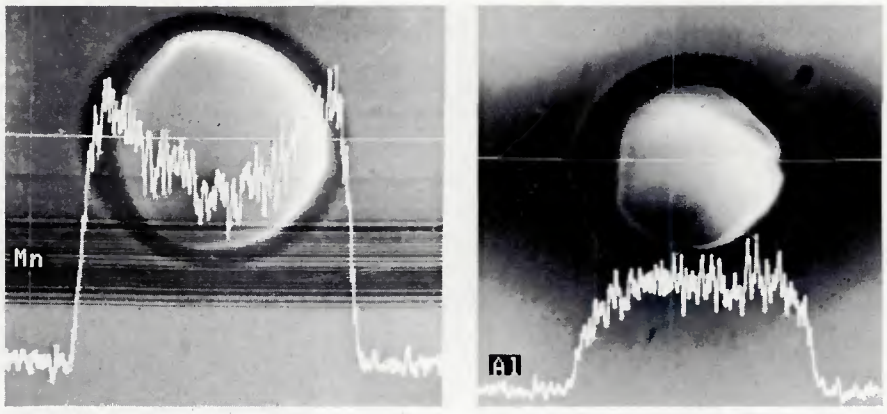

Fig. 1—Examples of x-ray line scan of elements of an inclusion found in a droplet deposited with Flux B at 600 A

welding are given in Tables 5 (300 A) and 6 (600 A). Both the total and inclusion Al and Mn analyses are reported in these two tables. The values for the inclusion analysis have been calculated from the total oxygen values given in the previous study (Ref. 1) and reproduced in Tables 5 and 6, and from the composition of the inclusions and relative abundance of Type 1 and Type 2 inclusions taken from Tables 2 and 3. By evaluating the data in this way, the relative amounts of Mn and Al in solution at the different stages of welding can be estimated. Although there is a degree of uncertainty in those calculations, because of the compounded errors in each of the individual chemical measurements, the scatter within the data, and the approximation that Type 1 and 2 inclusions account for the total O measured, nevertheless, some important qualitative observations can be made. For example, it is clear that, for Fluxes L1 through L4, significant amounts of Al remain in solid solution after deoxidation at the electrode tip and droplet stages. But at the weld metal stage, the majority, if not all, of the Al is tied up in the form of inclusions. For Flux L5, which contained only CaF_2 and CaO, there is negligible change in the Al content at all stages. The magnitude of the welding current had little or no effect on the results, other than a small increase in the oxygen levels at the higher current of 600 A.

The flux composition clearly is the single most important factor in determining the trends shown by the data in Tables 5 and 6. For example, the change in Mn levels at the tip and droplet stages correlates with the MnO content of the flux. The flux composition factor can also be observed by comparing the aluminum level at the tip stage between the case when Flux L5 was used and when the other fluxes were used. Flux L5 contained no Al_2O_3, and the resulting aluminum level at the tip stage is less than when the other fluxes were used. The variation of aluminum level when Fluxes L1 and L4 were used showed that other factors, such as activity, rather than a straightforward weight-percentage composition, are necessary to explain the results.

Dilution Factors

The dilution factors were estimated from metallographic cross-sections of the welds. The weld profiles observed were similar for the welding condition employed, except that at higher current, the depth-to-width ratio is marginally higher. The dilution factor, as shown in Table 7, only varied from 51% to 57%.

Discussion

Inclusion Analysis

Consideration of the chemical composition of the inclusions provides some information pertaining to the origin of the inclusions. The large size of many of the inclusions (up to 100 μm in diameter at the electrode tip and metal droplet stages) might suggest that they were formed by entrapment of molten flux particles. However, at the electrode tip and droplet stages, the majority of the large inclusions contained no CaO, whereas all the fluxes contained approximately 40 wt-% CaO. This is particularly noticeable for Flux L1 when welding at 300 A, where no CaO-containing inclusions were found in either the electrode tip or weld metal droplets. Even with those inclusions that contained CaO, there was considerable variability in their chemical composition (see, *e.g.*, the data in Table 4), and this, coupled with the composition profiles in individual inclusions (Fig. 1), points to extensive reactions prior to freezing. The reactions concerned are those between deoxidizers and oxygen. From the relative changes of oxygen, aluminum and manganese at the electrode tip and droplet stages, it is clear that flux decomposition is the major source of these deoxidizers and oxygen.

There is no doubt that some of the Ca-containing inclusions originated from flux entrapment. The extent of entrapment may depend on the relative stability of the arc. However, from the number of these Ca-containing inclusions, and more importantly, from the considerably modified composition of the inclusions, it can be concluded that flux entrapment is not a major source of oxygen.

There are, however, other possible mechanisms whereby Ca could be transferred from flux to metal. Although CaO is one of the most stable oxides, the maximum temperatures in the arc cavity are sufficiently high (in excess of 10,000°C/18,032°F) that partial decomposition of all oxide species would be anticipated. At the weld pool stage, it is easy to see how slag particles are carried into the weld pool due to the turbulence generated by the metal droplets. These slag particles will react extensively with the weld metal and form a basis for the growth of inclusions as the pool cools down. This could explain how CaO-containing inclusions formed at the weld metal stage with Fluxes L1 and L5, while none were observed at the earlier droplet stage on welding at 300 A—Table 2. Since the oxygen levels of these two welds were quite low, no nucleation in the weld pool occurred, resulting in the observation that all inclusions contained CaO. On the other hand, when Fluxes L2 through L4 were used, the higher oxygen level led to frequent nucleation in the weld pool, forming inclusions containing no CaO.

Fluxes L1 and L5 contain CaF_2, and reactions involving CaF_2 may occur (Refs. 10, 11) between the metal-slag interfaces of the slag droplets drawn into the weld pool, such as follows:

$$3\,CaF_2 + Al_2O_3 \rightleftharpoons 3\,CaO + 2\,AlF_3\,(g) \quad (1)$$

$$3\,CaF_2 + 2\,\underline{Al} + 3\,\underline{O} \rightleftharpoons 3\,CaO + 2\,AlF_3\,(g) \quad (2)$$

$$2\,CaF_2 + \underline{Si} + 2\,\underline{O} \rightleftharpoons 2\,CaO + SiF_4\,(g) \quad (3)$$

Reaction 1 may also occur within the slag phase. This led to a second important trend shown by the compositional data in Tables 2 and 3, which is the clear difference in behavior for Fluxes L2 through L4 on the one hand, and L1 on the other. In the former case, while there were variations with flux type, all the inclusions contained varying amounts of Al_2O_3 (for Fluxes L2 through L4), MnO and SiO_2 at all three stages. In the latter case, the composition of inclusions when using Flux L1 (containing CaO, CaF_2 and Al_2O_3) differed markedly at the weld metal stage from that at the earlier stages. With Flux L1, the inclusions at the first two stages were predominantly of the manganese silicate type, while at the weld metal

Table 5—Analysis of Al, Mn, Si and O at Different Stages of Welding (at 300 A)

	Tip					Droplet					Weld Metal					
	Al (wt-%)		Mn (wt-%)		O	Al (wt-%)		Mn (wt-%)		O	Al (wt-%)		Mn (wt-%)		O	Si (wt-%)
	Total	Inclusion	Total	Inclusion	(wt-%)	Total	Inclusion	Total	Inclusion	(wt-%)	Total	Inclusion	Total	Inclusion	(wt-%)	Total
Flux																
L1	0.017	0.003	0.82	0.11	0.88	0.164	0.014	0.58	0.15	0.141	0.032	0.024	1.28	0.002	0.026	0.09
L2	0.030	0.011	1.00	0.15	0.143	0.130	0.042	1.55	0.40	0.245	0.006	0.004	2.40	0.12	0.062	0.07
L3	0.036	0.008	0.90	0.10	0.098	0.051	0.026	0.61	0.17	0.174	0.032	0.022	1.34	0.03	0.057	0.40
L4	0.047	0.012	1.06	0.15	0.142	0.085	0.049	1.09	0.18	0.219	0.014	0.010	2.16	0.05	0.051	0.21
L5	0.003	0.000	0.73	0.08	0.093	0.001	0.000	0.59	0.27	0.247	0.004	0.004	1.04	0.03	0.036	0.04

Table 6—Analysis of Al, Mn and O at Different Stages of Welding (at 600 A)

	Tip					Droplet					Weld Metal				
	Al (wt-%)		Mn (wt-%)		O	Al (wt-%)		Mn (wt-%)		O	Al (wt-%)		Mn (wt-%)		O
	Total	Inclusion	Total	Inclusion	(wt-%)	Total	Inclusion	Total	Inclusion	(wt-%)	Total	Inclusion	Total	Inclusion	(wt-%)
Flux															
L1	0.055	0.001	0.038	0.13	0.100	0.152	0.015	0.61	0.16	0.150	0.034	0.022	1.30	0.00	0.027
L2	0.061	0.024	1.08	0.15	0.137	0.136	0.038	1.54	0.26	0.265	0.007	0.007	2.24	0.11	0.072
L3	0.038	0.027	1.00	0.10	0.117	0.079	0.027	0.61	0.11	0.182	0.030	0.016	1.32	0.03	0.054
L4	0.059	0.030	1.11	0.16	0.166	0.076	0.040	1.04	0.17	0.220	0.019	0.011	1.93	0.05	0.058

stage, they were alumina (with some dissolved CaO in the Type 1 inclusions). This again suggests that some particular reaction involving CaF_2 and Al_2O_3 is important for this flux.

The chemical composition of the inclusions formed at the electrode tip and in the metal droplets are not those which might be anticipated from the overall composition of the metal. As Tables 5 and 6 demonstrate, significant quantities of Al remain in solution, yet Al_2O_3 was usually the minor component in the inclusion composition. This is probably a consequence of the highly nonequilibrium conditions which pertain during the freezing of the metal, as shown by the Al and Mn profiles observed within the large inclusions – Fig. 1. In this case, the ability of the inclusion to maintain equilibrium with the metal as the temperature decreases is limited by the supply of Al to the growing inclusion, with the result that the inclusion is richer in Mn and Si and leaner in Al. This behavior can be compared to the weld metal situation where, as mentioned previously, most, if not all, of the Al has been removed from solution. The time for freezing is of course much longer for the weld metal than for either the electrode tips or the droplets.

Reactions within the Arc Column

Since the data for the behavior of Al and Mn were very similar at 300 and 600 A, this discussion will be confined to the observations pertaining to 300 A. Table 8 summarizes the trends observed for the five fluxes for the elements Al, Mn and O (the oxygen data are taken from Table 5 in Ref. 1). Fluxes L1 through L4 all show a gain of Al at both the electrode tip and droplet stages, this gain being greatest for Flux L1 and least for L3. With Flux L5, which contained no Al_2O_3, there was an apparent small loss of Al or Al_2O_3 at both stages. For Fluxes L1 to L4, the increase in Al was predominantly in the solid solution form, as the analysis (Table 5) showed that Al combined in the form of inclusions ranged from a low figure of approximately 9% (L1, droplet) to a high value of 57% (L4, droplet) of the total Al content. This would imply that much of the increase in the Al content must come from decomposition of the flux with subsequent absorption of Al from the plasma that surrounds the metal droplets as they cross the arc column from electrode tip to weld pool. Support for this mechanism comes from the work of Chervonnyi, *et al.* (Ref. 12), who showed that the vapor species of Al_2O_3 effusing from a tungsten cell in the temperature range of 2300–2600 K included Al^+ and Al_2O^+ ions, as well as Al, Al_2O, AlO, Al_2O_3 and O. Above 4300 K, further dissociation of the molecular species occurs (Ref. 13), so that in the temperature range of 10,000–20,000 K (the arc welding plasma temper-

Table 7—Dilution Factors of Welds Estimated by Metallography

Flux	L1	L2	L3	L4	L5
300 A	56%	55%	54%	53%	57%
600 A	55%	53%	54%	51%	–

Table 8—Relative Changes in Al, Mn and O Contents (300 A data)

Flux	Element	Wire → Electrode Tip	Electrode Tip → Droplet	Droplet → Weld Metal[a]
L1	Al	+0.011	+0.147	−0.054
	Mn	−0.24	−0.24	+0.02
	O	+0.072	+0.053	−0.038
L2	Al	+0.024	+0.1	−0.066
	Mn	−0.06	+0.55	+0.72
	O	+0.128	+0.101	−0.050
L3	Al	+0.030	+0.015	−0.004
	Mn	−0.16	−0.29	+0.09
	O	+0.083	+0.076	−0.026
L4	Al	+0.041	+0.038	−0.039
	Mn	–	+0.03	+0.70
	O	+0.127	+0.077	−0.054
L5	Al	−0.003	−0.002	−0.001
	Mn	−0.33	−0.14	−0.23
	O	+0.077	+0.154	−0.072

[a]The calculation for this stage takes account of the dilution factor (Table 7) and the base plate composition (Table 1).

atures), aluminum and oxygen would be present in the arc column.

For the other Al_2O_3-bearing fluxes that did not contain CaF_2 (L2, L3, L4), the total amount of Al picked up from the electrode wire to weld metal droplets ranged from 0.045 wt-% for L3 and 0.079 wt-% for L4 to 0.124 wt-% for L2. These three fluxes contained approximately the same amount of Al_2O_3, but had varying SiO_2 and MnO contents. This order of ranking of the fluxes correlated with the total O pickup (Table 8), 0.159 wt-% for L3, 0.204 wt-% for L4 and 0.229 wt-% for L2, suggesting that the oxygen potential of the flux (Ref. 14) controls not only the total amount of O picked up in the arc column, but also the Al absorption. This observation is consistent with the conclusion in the previous study (Ref. 1) that flux decomposition is the major source of oxygen at the electrode tip and metal droplet stage. A more extensive dissociation of the flux not only supplies more oxygen, but also other species, such as aluminum. This conclusion is of course limited to the rather narrow range of flux compositions studied and does not consider the influence of reactions such as the one discussed below.

When Flux L1 was used, the Al picked up from the electrode wire to the weld metal droplets was significantly higher (0.158 wt-%), although the Al_2O_3 content of L1 was about the same and the oxygen level at this stage was lower than the other fluxes (L2, L3 and L4).

The additional factor, which would account for the marked increase in Al levels at the droplet stage, is reaction (1), above. One of the products of this reaction is gaseous AlF_3, which will decompose in the arc column and/or react with Si in the metal droplet according to the equation:

$$4\ AlF_3 + 3\ \underline{Si} \leftrightarrows 3\ SiF_4 + 4\ \underline{Al} \qquad (4)$$

This mechanism is consistent with the inclusion composition discussed above.

The behavior of Mn in the arc column is complicated by the competing reactions which involve this element, *viz.*, the loss of Mn from the droplet by evaporation or oxidation and the gain of Mn by decomposition of the flux. For the three fluxes which did not contain MnO, *i.e.*, L1, L3 and L5, only the factors that lead to a loss of Mn need be considered. The total Mn lost at the first two stages, *i.e.*, from the starting electrode wire composition (1.06 wt-% Mn) to the weld metal droplet, was very similar for all three fluxes: 0.48 wt-% (L1), 0.45 wt-% (L3) and 0.47 wt-% (L5). Thus, approximately 45% of the Mn content of the wire has been lost in a very short time interval, estimated to be 0.1 s, according to Pokhodnya and Kostenko (Ref. 15). It is interesting to compare this rate of loss with that which has been measured for levitated Fe-Mn droplets in inert gas atmospheres. Kim and McLean (Ref. 16) have shown that the rate of Mn evaporation is given by the relationship:

$$\ln \frac{(\%\ Mn)_t}{(\%\ Mn)_o} = \frac{-\ kA\ t}{V} \qquad (5)$$

where $(\%\ Mn)_o$ and $(\%\ Mn)_t$ are the initial Mn content and the Mn content at time t, respectively, A and V are the surface area and volume of the droplet, and k depends on temperature:

$$k = 2.73 \exp(-31870/RT)\ cm/s \qquad (6)$$

If this expression is used to evaluate the rate of Mn evaporation taking values of 20 cm^{-1} for A/V, *i.e.*, a spherical droplet, 3 mm (0.12 in.) in diameter (Ref. 1), 0.1 s for t, estimated from the work of Pokhodnya and Kostenko (Ref. 15), and a temperature of 2000°C (3632°F), we find that the predicted loss of Mn is about 30 times smaller than the observed loss. A number of factors could account for the much faster rates of Mn evaporation during welding. The assumed temperature of 2000°C (3632°F) may underestimate the actual metal temperatures, particularly in the transfer stage when the droplet is in contact with an extremely hot plasma. The observed loss could, in fact, be predicted from equations 5 and 6 if the temperature of the droplet was then 7200°C (12,992°F). A second important consideration is the role that oxygen plays in enhancing the rate of Mn evaporation. Disten and Whiteway (Ref. 15) have shown that at 1750°C (3182°F) oxygen accelerates the rate of evaporation of Fe over that found in an inert atmosphere by a factor of 10, when the partial pressure of oxygen is 10^{-2} atm. One would anticipate a similar enhancement for Mn evaporation rates.

With MnO-bearing fluxes, the rate of Mn evaporation is offset to a considerable extent by decomposition of the flux. For the two MnO levels used in this study, the 13 wt-% flux (L4) produced little change in the Mn content of the metal droplets, while the 25 wt-% flux (L2) transferred considerable Mn to the droplets, particularly during the free flight stage from electrode tip to the weld pool. From the relative amount of manganese and oxygen absorbed at this stage, it can be shown that the atomic ratio of Mn:O (1.6:1) is larger than the stoichiometric ratio of MnO. Thus, some of the manganese must be absorbed in the atomic form. This observation points to the importance of flux decomposition rather than flux entrapment as the major contributing factor to the reactions in the arc column.

Weld Pool Metal-Slag Reactions

For the range of flux compositions studied in this work, it has been shown that metal droplets entering the weld pool contain appreciable quantities of Al, Mn, Si and O in solution. In assessing the reactions that will be important in determining the final weld metal composition, and particularly the oxygen content, it is useful to divide these into three groups:

1. Deoxidation reactions of the type

$$x\underline{Al} + y\underline{Si} + z\underline{Mn} + \underline{O} \leftrightarrows > (Al_xSi_yMn_z)\ O \qquad (7)$$

where the underlined elements are dissolved in the molten steel and the product of deoxidation is a complex oxide. Such reactions will lead to a decrease in the total oxygen level only if the reaction products separate out into the slag phase.

2. Slag-metal reactions involving an exchange of elements such as Al, Mn and Si, but no change in the oxygen content of the weld:

$$3(MnO) + 2\ Al \leftrightarrows >3\ Mn + (Al_2O_3):\quad G = -112972 + 3.71\ T \qquad (8)$$

$$2(MnO) + Si \leftrightarrows >2\ Mn + (SiO_2):\quad G = -20518 - 4.82\ T \qquad (9)$$

$$3(SiO_2) + 4\ Al \leftrightarrows >3\ Si + 2\ (Al_2O_3):\quad G = -164390 + 21.88\ T \qquad (10)$$

The standard free energy changes accompanying these reactions are taken from Kubachewski and Alcock (Ref. 15) (units in cals). In addition to these three reactions, for Fluxes L1 and L5 the reactions involving CaF_2 discussed earlier (equations 1-3) fall into this category. Again, there is no net loss of oxygen unless the CaO subsequently separates into the slag layer.

3. Flux decomposition reactions:

$$(MnO) \leftrightarrows > Mn + O:\quad G^\circ = 58376 - 29.5\ T \qquad (11)$$

$$(SiO_2) \leftrightarrows > Si - 2\ O:\quad G^\circ = 137270 - 54.20\ T \qquad (12)$$

The reactions are favored by high temperatures and will be enhanced by high activities in the molten flux.

The relative importance of each of these reactions within the three groups can be assessed from the data in the last column of Table 8. With all five fluxes, there was a net loss of oxygen between the droplet and the weld metal stages, indicating that the formation and separation of oxide reaction products is an important process in determining the final weld metal oxygen levels. Several factors have an influence on this process: the density of the inclusions (Ref. 7), turbulence in the weld pool and the composition of the inclusions. Plockinger (Ref. 19) has shown that for efficient separation the interfacial tension between the inclusion and the molten steel should be as high as possible. He suggested that, for

this reason, alumina-rich inclusions separate out more efficiently than silica-rich inclusions. This could explain the observation that with Flux L1 the final oxygen values were considerably lower than those obtained with Flux L3, although the oxygen levels at the droplet stage were similar. The inclusions formed in the weld metal with Flux L1 contained no SiO_2, whereas with Flux L3 they contained approximately 30 wt-% SiO_2—Tables 2 and 3.

A comparison of the inclusion separation efficiency for Fluxes L2 and L4 is complicated by the manganese and oxygen pickup that could occur in reactions (8), (9) and (11). With each of these fluxes, there was a gain of approximately 0.7 wt-% manganese. This gain suggests more extensive slag-metal interactions and flux decomposition reaction than those occurring with Fluxes L1 and L3. However, there was still a net loss of oxygen, stressing the importance of the formation and separation of oxide products. The slag formed from Flux L5 was very fluid. This high fluidity made effective protection during metal droplet collection difficult. The consequent possibilities of contamination by the atmosphere led to an artificially high oxygen value in the droplets. Hence, the changes calculated between the droplet and weld metal stage could be inaccurate. While this inaccuracy does not affect the observed phenomenon, *i.e.,* separation of deoxidation products in the weld pool, which is similar for all fluxes, a definitive statement on the relative efficiency of inclusion separation with different fluxes cannot be made.

Chemical Equilibrium

In this section, consideration is given to the relevance of chemical equilibrium concepts with respect to metal-slag reactions during welding. For reasons discussed previously in this paper, such an approach would appear to be limited, particularly since it ignores many of the dynamic events that are important in determining final oxygen levels. Nevertheless, the concept of chemical equilibrium has been used by many authors in this field, and it is of interest to compare predicted equilibrium temperatures with those given elsewhere in the literature. In essence, this approach assumes that the measured values of the different species correspond to those that would have been in solution in iron at a particular temperature during the thermal cycle of the liquid weld metal. Any products of deoxidation formed at lower temperatures would have insufficient time to escape to the slag and would therefore be included in the analysis. Conversely, it is assumed that any deoxidation products formed above this temperature would be removed in the slag phase. The present results, particularly those related to the levels of Al and O, clearly show that there must be a reduction in the inclusion content before the weld freezes.

The free energy changes for the possible reactions have been taken from Kubachewski and Alcock (Ref. 18) and the interaction coefficients from Elliott (Ref. 21). The method of calculation is illustrated for Flux L1. In this case, the reaction defining equilibrium is taken to be:

$$2\,Al + 2\,O \rightleftharpoons Al_2O_3 \qquad (13)$$

for which

$$G^\circ = 288100 - 92.24\,T = RT\,\ln\frac{{}^{h}Al^{2}\,{}^{h}O^{3}}{{}^{2}Al_2O_3} \qquad (14)$$

The activity of Al_2O_3 in the flux is taken to be equal to the mole fraction of Al_2O_3, which in the case of Flux L1 is 0.27. h_1 and h_0 are the Henrian activities of Al and O, respectively, and are given by:

$$\log h_1 = (e)^{Al}_{Al}(\text{wt-\% Al}) + (e)^{S}_{Al}(\text{wt-\% Si}) + (e)^{C}_{Al}(\text{wt-\% O}) + \log(\text{wt-\% Al})$$

$$\text{and } \log h_0 = (e)^{O}_{O}(\text{wt-\% O}) + (e)^{S}_{O}(\text{wt-\% Si}) + (e)^{Al}_{O}(\text{wt-\% Al}) + \log(\text{wt-\% O})$$

where $(e)^{C}_{B}$ is an interaction coefficient expressing the influence of C on the behavior of B. Substituting the appropriate values in equation (14) yields a value for T of 2285 K.

For Flux L2, reactions (8), (11) and (13) are all possible equilibria. In this case, by following the same procedures outlined above, the effective reaction temperatures for these three reactions are 3160, 1900 and 2260 K, respectively. For Flux L3, activity data (Refs. 21, 22) are available at 1600°C (2912°F) for slags of similar composition. Using these data, values are obtained for a SiO_2 of 0.01 and an Al_2O_3 of 0.25. Using these activity values, effective equilibrium temperatures of 2400, 2340 and 2360 K are found for the reactions given by equations (10), (12) and (13), respectively.

For Flux L4, the activity coefficient of MnO in this slag has been estimated to be 2.5 at 1600°C (2912°F) (Ref. 23). Using this value, equilibrium temperatures of 2880 and 1840 K are calculated for reactions (8) and (11), respectively.

The effective reaction temperatures for the Al-Al_2O_3, Mn-MnO and Si-SiO_2 reactions are seen to all lie between 1840 and 2405 K, and straddle the values normally accepted for the effective weld pool temperature. Davis and Coe (Ref. 5), using data from Tuliani, *et al.* (Ref. 2), showed that the oxygen content of the weld metal corresponded to the equilibrium of the Fe-FeO reaction at 1923 K, while Eagar (Ref. 4) postulated that, for acidic fluxes, the effective equilibrium temperature was 2273 K. The value of 3160 K obtained for the equilibrium temperature for the MnO-Al reaction (Flux L2) is much higher than the other values. This might suggest that this reaction has not reached equilibrium, or that the values used for the activities of the components of this particular flux are in error.

The analysis of the results presented in this section suggests that a near equilibrium state may be attained at some stage during the thermal cycle of the weld pool. However, it must be emphasized again that in the last analysis it is the efficiency of inclusion separation that determines the final oxygen level in the weld metal.

Summary and Conclusions

In this study, the oxygen, aluminum and manganese contents, as well as the inclusion compositions at the electrode tip, metal droplet and weld metal stages, have been determined. With fluxes, wire and base plate of known compositions, and from the relative changes from one stage to another, it was possible to assess and evaluate the different types of reactions occurring during the weld process and to identify the major factors which control the final oxygen level in the weld metal. The following points summarize the observations:

1. The electrode tip and metal droplet stage are the major sites for oxygen absorption. Determination of aluminum and manganese level, as well as the composition of inclusions, showed that the major source of oxygen is decomposition of the flux.

2. It was found that a significant portion of the aluminum absorbed in the electrode tip and droplet stages was in the solid solution form, *i.e.,* a non-oxidized form. This implied extensive decomposition of flux components within the arc column.

3. At the weld metal stage, metal-slag reactions may or may not occur. In this study, it was found that fluxes containing MnO showed significant metal-slag reactions, while MnO-free fluxes did not.

4. Significant loss of oxygen, as well as metallic species such as aluminum, at the weld metal stage indicated separation of oxidation products as the most significant factor determining the final oxygen content.

5. A near equilibrium state may be attained at some stage during the thermal cycle of the weld pool; however, it is the efficiency of inclusion separation that determines the final oxygen level in the weld metal.

Acknowledgments

The authors are grateful to the Department of Energy, Mines and Resources

and N.S.E.R.C., Canada, for support of this work, and to Alcan for the award of a research fellowship to T. W. Lau.

References

1. Lau, T., Weatherly, G. C., and McLean, A. 1985. The sources of oxygen and nitrogen contamination in submerged arc welding using CaO-Al_2O_3 based fluxes. *Welding Journal* 64(12):343-s to 347-s.

2. Tuliani, S. S., Boniszewski, T., and Eaton, N. F. 1969. Notch toughness of commercial submerged arc weld metal. *Welding and Metal Fabrication* (8):327.

3. North, T. H., Bell, H. B., Nowicki, A., and Craig, I. 1978. Slag/metal interaction, oxygen and toughness in submerged arc welding. *Welding Journal* 57(3):63-s to 75-s.

4. Eagar, T. W. 1978. Sources of weld metal oxygen contamination during submerged arc welding. *Welding Journal* 57(3):76-s to 80-s.

5. Davis, M. L. E., and Coe, P. R. 1977. Welding Institute Research Report 39/1977/M, British Welding Institute, Cambridge, England.

6. Caryll, D. B., and Ward, R. C. 1967. Study of slag-metal equilibria by levitation melting application to the Fe-Mn-O system. *Journal of Iron and Steel Institute* 205:28.

7. Tuliani, S. S., Boniszewski, T., and Eaton, N. F. 1972. Carbonate fluxes for submerged arc welding of mild steel. *Welding and Metal Fabrication* (7):247.

8. Erokhin, A. A., and Baikor, A. A. 1960. Effect of welding condition variables on interaction between deposited metal and gases and slag in arc welding. *Automatic Welding* (5):1.

9. Potapov, N. N., and Lyubavskii, K. V. 1971. Interaction between the metal and slag in the reaction zone during submerged arc welding. *Welding Production* (7):14.

10. Mitchell, A. 1967. Transcript Faraday Society 63:153.

11. Kay, D. A. R. Aug. 1967. International symposium on electroslag consumable, electrode melting and casting technology. Pittsburg, Pa., p. 55.

12. Chervonnyi, D. A., Kashereninov, O. E., and Manelis, G. B. 1977. Mass-spectrometric investigations of gas-phase equilibria over Al_2O_3 at high temperatures. *High Temperature Science* 9:99.

13. Rains, R. K., and Kadlec, R. H. 1970. The reduction of Al_2O_3 to aluminum in a plasma. *Metallurgical Transactions* 1 (4-6):1501.

14. Davis, M. L. C., and Bailey, N. 1980. *Weld Pool Chemistry and Metallurgy*. British Welding Institute, Cambridge, England, p. 255.

15. Pokhodnya, J. K., and Kostenko, B. A. 1965. Fusion of electrode metal and its interaction with the slag during submerged arc welding. *Automatic Welding* 18(10):16.

16. Kim, C. K., and McLean, A. To be published.

17. Disten, P. A., and Whiteway, S. G. 1970. Kinetics of vapourization and oxidation of liquid iron levitated in glowing helium-oxygen. *Canadian Metallurgical Quarterly* 9:419.

18. Kubachewski, O., and Alcock, C. B. 1979. *Metallurgical Thermochemistry*. Pergamon Press.

19. Plockinger, E. 1963. Influence of deoxidation practice on cleanness of steel. *Journal of Iron and Steel Institute* 201:576.

20. Elliott, J. F. 1963. *Thermochemistry for Steelmaking*. Addison-Wesley.

21. Chipman, J. 1961. Physical chemistry of process metallurgy. P. I., New York—London, p. 27.

22. Kay, D. A. R., and Taylor, J. 1960. Transcript Faraday Society 56:139.

23. Abraham, K. P., Davis, M. W., and Richardson, F. D. 1960. *Journal of Iron and Steel Institute* 196:182.